THERMAL CYCLING RELIABILITY OF CHIP RESISTOR LEAD FREE SOLDER JOINTS

Jeffrey C. Suhling, H. S. Gale, R. Wayne Johnson, M. Nokibul Islam, Tushar Shete, Pradeep Lall, Michael J. Bozack, John L. Evans
Center for Advanced Vehicle Electronics (CAVE)
Auburn University
Auburn, AL 36849
Phone: (334) 844-3332
Fax: (334) 844-3307
Email: jsuhling@eng.auburn.edu

Ping Seto, Tarun Gupta, James R. Thompson
DaimlerChrysler - Huntsville Electronics
100 Electronics Boulevard
Huntsville, AL 35824

ABSTRACT

The solder joint reliability of ceramic chip resistors assembled to laminate substrates has been a long time concern for systems exposed to harsh environments such as those found in automotive and aerospace applications. This is due to a combination of the extreme temperature excursions experienced by the assemblies along with the large coefficient of thermal expansion mismatches between the alumina bodies of the chip resistors and the glass-epoxy composites of the printed circuit boards (PCBs). These reliability challenges are exacerbated for components with larger physical size (distance to neutral point) such as the 2512 resistors used in situations where higher voltages and/or currents lead to power dissipations up to 1 Watt. In this work, the thermal cycling reliability of several 2512 chip resistor lead free solder joint configurations has been investigated. In an initial study, a comparison has been made between the solder joint reliabilities obtained with components fabricated with both tin-lead and pure tin solder terminations. In the main portion of the reliability testing, two temperature ranges (-40 to 125 ^{o}C and -40 to 150 ^{o}C) and five different solder alloys have been examined. The investigated solders include the normal eutectic SnAgCu (SAC) alloy recommended by earlier studies (95.5Sn-3.8Ag-0.7Cu), and three variations of the lead free ternary SAC alloy that include small quaternary additions of bismuth and indium to enhance fatigue resistance. For each configuration, thermal cycling failure data has been gathered and analysed using two-parameter Weibull models to rank the relative material performances. The obtained lead free results have been compared to data for standard 63Sn-37Pb joints. In addition, a second set of thermally cycled samples was used for microscopy studies to examine crack propagation, changes in the microstructure of the solders, and intermetallic growth at the solder to PCB pad interfaces.

INTRODUCTION

Legislation that mandates the banning of lead in electronics, due to environmental and health concerns, has been actively pursued in several countries during the past 15 years. Although the products covered by and implementation deadlines for such legislation continue to evolve, it is clear that laws requiring conversion to lead-free electronics are becoming a reality. Other factors that are affecting the push towards the elimination of lead in electronics are the market differentiation and advantage being realized by companies producing so-called “green” products that are lead-free. A large number of research studies have been performed and are currently underway in the lead-free solder area. Detailed reports on multi-year studies have been published by the National Center for Manufacturing Sciences (NCMS) and the National Electronics Manufacturing Initiative (NEMI), as well as other consortia. Although no “drop in” replacement has been identified for all applications; Sn-Ag, Sn-Ag-Cu (SAC), and other alloys involving elements such as Sn, Ag, Cu, Bi, In, and Zn have been identified as promising replacements for standard 63Sn-37Pb eutectic solder.

There have been many reports that solder joint reliability can actually be increased for a given application by using a lead-free replacement alloy such as Sn-Ag-Cu instead of conventional Sn-Pb. However, this conclusion is not universal, and the degree of reliability improvement or degradation is package/design and environment dependent. In thermal cycling reliability environments, Sn-Ag-Cu alloys appear to often outperform Sn-Pb. This has been found for solder joints in more compliant package-board assemblies such as leaded components (e.g. QFPs) and Plastic Ball Grid Array (PBGA) applications [1], and also for more stiff components (CBGA) subjected to small temperature changes [2]. However, for very stiff components with a high coefficient of thermal expansion (CTE) mismatch with the substrate (e.g. CBGA on FR-4, and non-underfilled flip chip on laminate), the solder joint reliability is typically poorer for lead-free Sn-Ag-Cu alloys in thermal cycling tests with large swings between the temperature extremes [3-4].

Another common Surface Mount Technology (SMT) configuration involving stiff components with high CTE mismatch to the substrate is the use of ceramic (alumina) bodied chip resistors on organic substrates (e.g. glass-epoxy laminates). The solder joint reliability of such components has been a long time concern for harsh environments with extreme temperature excursions, such as those found in automotive and aerospace applications. These reliability challenges are further exacerbated for components with larger physical

size (distance to neutral point) such as the 2512 resistors used in situations where higher voltages and/or currents lead to power dissipations up to 1 Watt.

Crack growth and the resulting shear strength degradation for both Sn-Ag-Cu and Sn-Pb-Ag chip resistor solder joints have been examined during thermal cycling [5]. It was found that the fatigue resistances between lead bearing and SAC solder joints were not significantly different, but were influenced by the component type and board metallization. In addition, crack length variation has been measured in chip capacitor solder joints as a function of thermal cycling [6]. Cracks were found to grow fastest in the Sn-Pb-Ag solder joints relative to several lead free alternatives. Finally, the changes in microstructure occurring in Sn-Ag-Cu chip resistor solder joints during thermal cycling have been recently examined [7]. A power law relationship was established between the number of cycles to crack initiation and the average β-Sn phase growth parameter.

In this work, the thermal cycling reliability of several 2512 chip resistor lead free solder joint configurations has been investigated. In an initial study, a comparison was made between the solder joint reliabilities obtained with components fabricated with both tin-lead and pure tin solder terminations. In the main portion of the reliability testing, two temperature ranges (-40 to 125 ^{o}C and -40 to 150 ^{o}C) and five different solder alloys have been examined. The investigated solders include the normal eutectic SnAgCu (SAC) alloy recommended by earlier studies (95.5Sn-3.8Ag-0.7Cu), and three variations of the lead free ternary SAC alloy that include small quaternary additions of bismuth and indium to enhance fatigue resistance. For each configuration, thermal cycling failure data has been gathered and analysed using two-parameter Weibull models to rank the relative material performances. The obtained lead free results have been compared to data for standard 63Sn-37Pb joints. In addition, a second set of thermally cycled samples was used for microscopy studies to examine crack propagation, changes in the microstructure of the solders, and intermetallic growth at the solder to PCB pad interfaces.

TEST BOARD

A test board was developed for examining the thermal cycling reliability of five sizes of chip resistors (2512, 1206, 0805, 0603, 0402). The industry standard naming convention for these chip resistor sizes describes the length and width of the resistor body in hundredths of an inch. For example, the 2512 resistor has a nominal length of .25 inches (6.35mm), and a nominal width of .12 inches (3.05mm). Each board contained 15 of each of the 5 sizes of chip resistors. The 15 resistors in each size were accessible electrically as 3 daisy-chain sets (5 resistors and thus 10 solder joints per chain). The resistor daisy chains were routed to plated through holes at the edge of the board where soldered wire connections could be made for use in resistance monitoring during the thermal cycling tests. Figure 1 is a photograph of an assembled test board. The fabricated test boards included four copper conductor layers, FR-406 glass/epoxy laminate material and had a thickness of 1.57 mm. The external copper traces had either a Hot Air Solder Leveled (HASL) Sn-Pb or an Electroless Nickel Immersion Gold (ENIG) finish. Figure 2 shows a top view of one of the 2512 resistors and a typical uncycled solder joint cross-section.

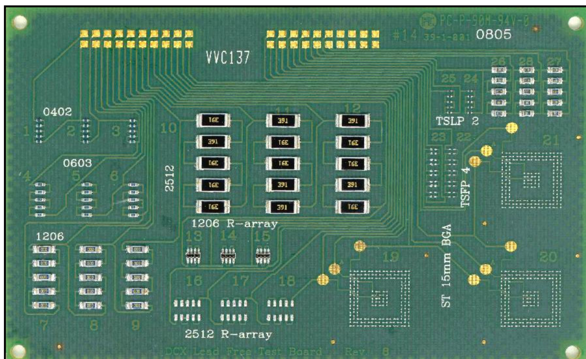

Figure 1 - Chip Resistor Test Board

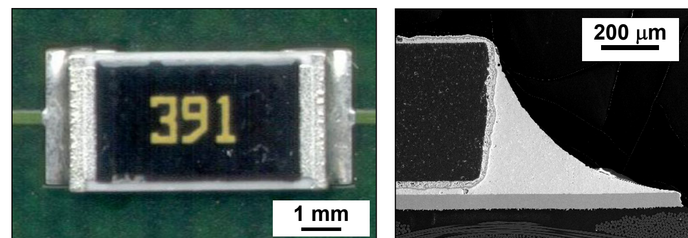

Figure 2 - 2512 Resistor Top View and Solder Joint

RELIABILITY TESTING

Thermal cycling (-40 to 125 ^{o}C and -40 to 150 ^{o}C) of the assembled test boards was performed in a pair of Blue-M environmental chambers, and 6000 cycles were completed for each temperature range before the testing was terminated. The thermal cycle duration was 90 minutes, with 30 minutes at each extreme. Typical thermocouple results from under a component on one of the test boards are illustrated in Figure 3. Enough boards were assembled so that each of the various legs of the test matrix had 12 test boards (36 resistor chains for each component size). The boards were placed vertically in the chamber, and the wiring passed through access ports to a data acquisition system. Monitoring of the various daisy chain networks was performed throughout the cycling using a high accuracy digital multimeter coupled with a high performance switching system controlled by LabView software. Failure of a daisy-chain network was defined as the point when the resistance change exceeded 5Ω.

RELIABILITY DATA

In this paper, only results for the 2512 resistor solder joint reliability will be discussed. Of all the tested chip components, the 2512 resistors have the largest body size and highest rated power dissipation, and consequently the poorest solder joint reliability. For those components with sufficient failures after 6000 cycles, the resulting failure data were statistically analysed using two parameter Weibull models. The standard parameters in such an approach are the Weibull Slope β, and the Characteristic Life η, which is the number of

cycles required to cause failure of 63.2% of the samples from a particular leg of the test matrix. From these values for a particular chip resistor configuration, the cumulative failures (percent) after any number of thermal cycles can be predicted.

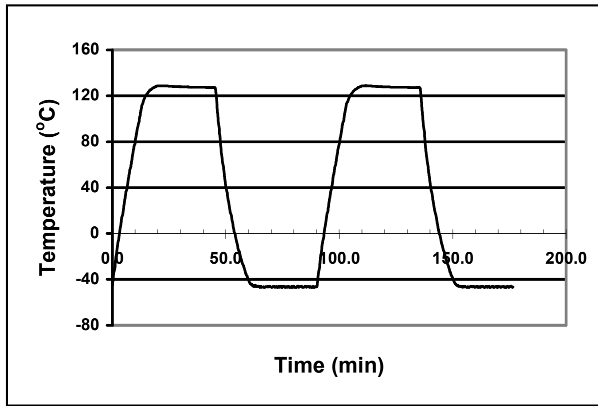

Figure 3 - Test Board Thermal Cycle (-40 to 125 ^{o}C)

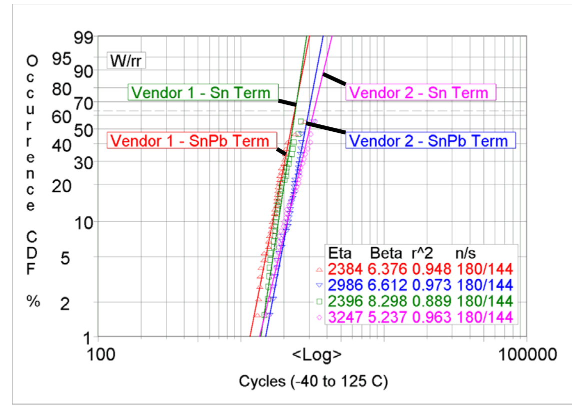

Figure 4 - Weibull Plot for Resistor Termination Study

Resistor Termination Study

Prior to studying the reliability differences between the various solder types, an initial investigation was performed to examine the effects of using different termination materials for the chip resistors. Historically, chip resistors have been fabricated with 90Sn-10Pb solder terminations to better match the Sn-Pb solder paste used in conventional SMT assembly and to avoid fillet lifting. However, a transition to pure Sn terminations has occurred as a part of the overall lead free initiative. In the resistor termination study performed here, 2512 resistors from two vendors, with both Sn-Pb and Sn terminations were considered. The boards were fabricated with a Sn-Pb HASL finish, and eutectic 63Sn-37Pb solder paste was utilized. Thus, the only lead-free attributes of these particular experiments were the Sn-terminations in some of the chip resistors. The Weibull failure plot for the Sn and Sn-Pb terminated chip components is shown in Figure 4. From these data, it can be seen that there was little difference in the failure data for the two termination types for a given resistor vendor, although the parts from vendor 2 consistently outperformed those from vendor 1. The nature of these reliability differences for the parts from the two vendors has yet to be explained. In all future discussions in this paper, resistors from vendor 2 with pure Sn termination were utilized.

Lead Free Alloy Study

The compositions of the five alloys (four lead free and standard 63Sn-37Pb) tested in this investigation are tabulated in Table 1. The lead free solders consisted of the standard SAC eutectic (95.5Sn-3.8Ag-0.7Cu) that is often recommended as a leading candidate for replacement of Sn-Pb, and a set of three quaternary Sn-Ag-Cu-X alloys, with either Bi or In as the fourth ingredient. The test boards utilized in this part of the investigation were fabricated with an Electroless Nickel Immersion Gold (ENIG) finish.

Table 1 - Solder Alloy Compositions

Alloy	Composition
Sn-Pb	63Sn-37Pb
Sn-Ag-Cu	95.5Sn-3.8Ag-0.7Cu
Sn-Ag-Cu-Bi (1)	92.35Sn-3.35Ag-1.0Cu-3.3Bi
Sn-Ag-Cu-Bi (2)	93.5Sn-3.8Ag-0.7Cu-2.0Bi
Sn-Ag-Cu-In	88.5Sn-3.0Ag-0.5Cu-8.0In

Typical thermal cycling reliability data for the 2512 resistor solder joints are shown below in Figures 5-7. In Figures 5 and 6, the reliabilities of 63Sn-37Pb and 95.5Sn-3.8Ag-0.7Cu solder joints are compared for the -40 to 125 ^{o}C and -40 to 150 ^{o}C temperature ranges, respectively. It can be seen from Figure 5, that the reliabilities are very similar for the -40 to 125 ^{o}C thermal cycling range. However, Figure 6 indicates that 63Sn-37Pb dramatically outperforms the lead free Sn-Ag-Cu alloy for the more extreme -40 to 150 ^{o}C testing. This result agrees with the earlier observations for non-underfilled flip chip on laminate assemblies [3-4], and further underscores the need to be cautious when proposing lead-free solder substitutions for SMT configurations including stiff components on organic laminate substrates where there are harsh environments with large temperature swings (e.g. automotive under-the-hood applications).

In the case of cycling from -40 to 125 ^{o}C, the reliabilities of the three quaternary Sn-Ag-Cu-X alloys were found to be the same or slightly lower than that of eutectic 95.5Sn-3.8Ag-0.7Cu. However, as shown in Figure 7, the addition of either Bi or In to Sn-Ag-Cu can significantly enhance the reliability of the lead free joints when exposed to the harsher -40 to 150 ^{o}C temperature range, where Sn-Ag-Cu performs poorer than standard Sn-Pb. Further investigation is required in order to determine the Sn-Ag-Cu-X lead free alloy formulation that best optimizes reliability in harsh environments.

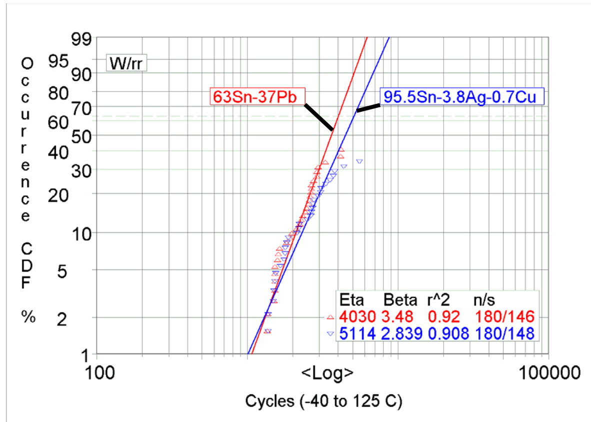

Figure 5 - Weibull Plot for 2512 Chip Resistors with Sn-Pb and Sn-Ag-Cu Solders (-40 to 125 ^{o}C)

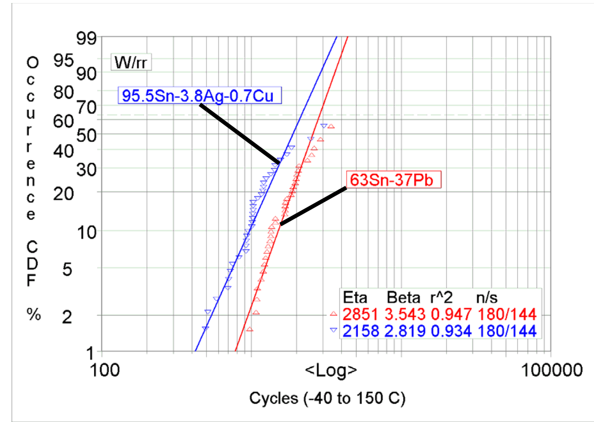

Figure 6 - Weibull Plot for 2512 Chip Resistors with Sn-Pb and Sn-Ag-Cu Solders (-40 to 150 ^{o}C)

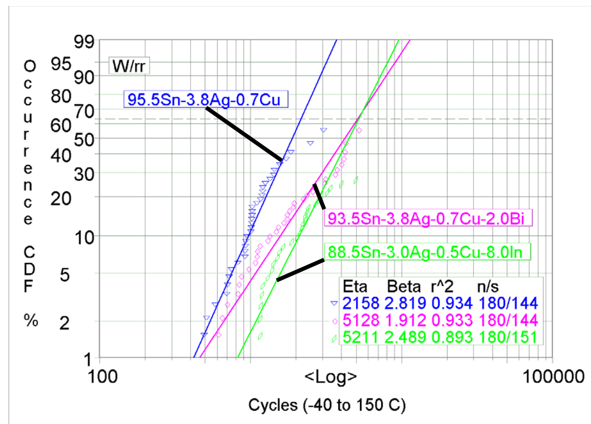

Figure 7 - Weibull Plot for 2512 Chip Resistors with Lead Free Solders (-40 to 150 ^{o}C)

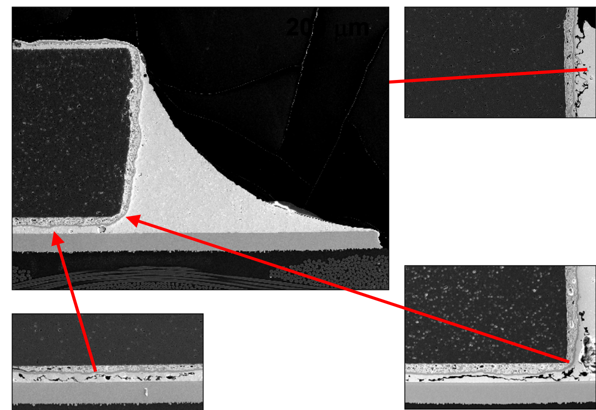

Figure 8 - Photograph of an Uncycled 95.5Sn-3.8Ag-0.7Cu Solder Joint with Images and Locations of Crack Initiation, Corner Turning, and Completion Selected from Various Cycled Samples

MICROSCOPY AND FAILURE ANALYSIS

Experimental Techniques

Metallographic samples were prepared from cross-sections of a set of supplemental boards subjected to various levels of thermal cycling. The cross-sections were characterized by scanning electron microscopy (SEM) using a JEOL JSM 840 instrument operated at an accelerating voltage of 20 kV. All samples were imaged as polished. The intermetallic phases observed in these joints were noticeably harder than the matrix. Thus, it was possible to obtain topographic contrast in secondary electron images (SEIs) of the polished samples without resort to etching. Backscattered electron images (BEIs) were also used to produce atomic number contrast (phases with a high average atomic number appear bright). Compositional data was obtained using energy dispersive x-ray spectroscopy (EDS) via an Oxford ultrathin window (UTW) detector and ISIS analyzer attached to the JSM 840.

Crack Propagation

Preliminary failure analysis has shown that the solder joint cracking and creep-fatigue damage propagates as expected for chip resistors on FR-4 substrates. As shown in Figures 8-9, cracks begin underneath the component and then typically follow along a path that parallels the resistor termination, turning the corner at the resistor edge, and then proceeding until complete separation has occurred. Unfortunately, insufficient cross-sections were made to fully characterize the crack growth for the various solders. In particular, the Weibull plots in Figures 5-7 indicate that many more cross-sections with environmental exposures between 500 and 3000 cycles would be necessary to develop a crack propagation criterion for the 2512 resistor solder joints. Another finding was that more study is needed to optimize the assembly process and reflow profile for each lead free solder type so that voids (see Figure 10) are minimized in the solder joints.

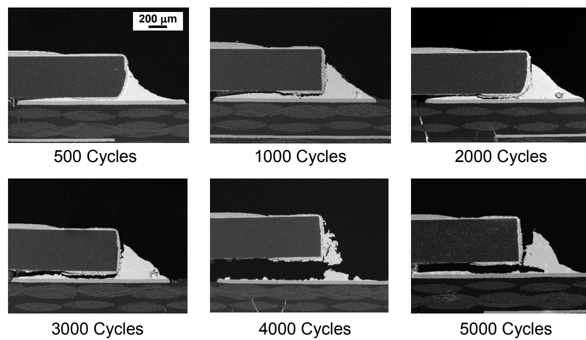

Figure 9 - Observed Cracks in 95.5Sn-3.8Ag-0.7Cu Joints After Various Numbers of Thermal Cycles (-40 to 150 ^{o}C)

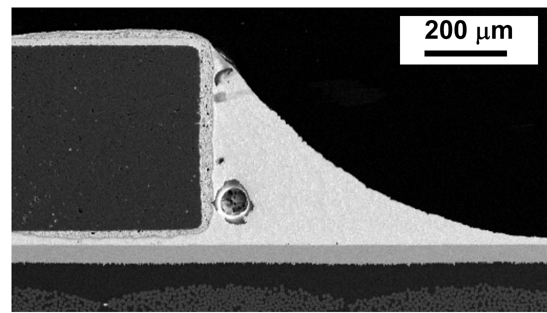

Figure 10 - Chip Resistor Lead Free Solder Joint with Void

Solder Fillet Microstructures

Example secondary electron images for the lead free solder joints that were cross-sectioned after various levels of thermal cycling from -40 to 150 ^{o}C are shown in Figures 11-12. In all cases, the magnified images were taken at the interface of the solder and PCB pad with ENIG plating finish, in the bulk of the joint but near the corner of the resistor termination. For all four of the lead free systems, a noticeable feature was that spheroidizing of the eutectic was observed to progress rapidly during cycling. Such spheroidization is driven by the energy of the interfaces between the phases making up the eutectic, since spheroidization reduces the total interfacial area and hence total interfacial energy. Spheroidization depends on diffusion transport, and would therefore have occurred during the hot part of the thermal cycles.

By changing the distribution of hard, brittle intermetallics, spheroidization can often have a significant effect on the mechanical properties of eutectic microstructures. For example, spheroidization can break up networks of brittle phases that would otherwise act as a continuous path for crack propagation. Spheroidization, does not involve a phase transformation, but simply a morphological change. However, this does not preclude the possibility of phase transformations occurring simultaneously with spheroidization. In the present study, it was difficult to determine if such transformations had occurred, due to the small size of some of the particles involved, which were below the spatial resolution of EDS (typically ~ 1 mm). Also, the apparent compositions of the larger particles, whose composition could be determined using EDS, did not tie up with the limited available phase diagrams. Identification of subtle microstructural changes would require the use of transmission electron microscopy (TEM) for microstructural characterization, which was not practicable given the large number of samples involved.

Spheroidization commenced quickly and was clearly apparent in all samples after only 500 cycles. There were variations in the extent of spheroidization within each alloy and an unequivocal difference in spheroidization from alloy to alloy was not apparent. Based on the results discussed above, differences in the gross fillet microstructure alone would not seem to account for the marked differences in thermal fatigue performance of the alloys studied.

Intermetallic Layers

The formation of distinct intermetallic layers was observed at the interfaces with the solders as seen in Figures 11-12. Use of x-ray elemental mapping techniques has shown that the copper and nickel layers largely remained on the surface of the PCB, because the intermetallic layer acted to some extent as a diffusion barrier. Nonetheless, sufficient copper and nickel diffused into the solder to form a variety of fine (a few mm in diameter) second phases throughout the fillets in all of the systems studied, as illustrated in the backscattered electron images in Figure 13.

A distinct difference between the alloys studied was the nature of the intermetallic layers (see Figures 11-12) during cycling from -40 to 150 ^{o}C. The intermetallic layers in the 95.5Sn-3.8Ag-0.7Cu alloy and the two Sn-Ag-Cu-Bi alloys were fairly fine (typically around 1-3 mm thick) and continuous. In contrast, the Sn-Ag-Cu-In alloy produced a highly irregular intermetallic layer consisting of large (10-20 mm) angular precipitates (see Figure 12). An unequivocal compositional difference could not be confirmed between the intermetallic layers formed in these different alloys. This analysis was complicated by EDS spot-size issues (see above) and overlaps between the In and Sn x-ray peaks. Since the 88.5Sn-3.0Ag-0.5Cu-8.0In alloy performed best in the -40 to 150 ^{o}C thermal cycling testing, and the 95.5Sn-3.8Ag-0.7Cu the worst, the size and morphology of these intermetallics could be the reason for the observed differences in performance between these alloys. However, a clear correlation was not observed between the performance of the various alloys investigated and any single microstructural feature.

SUMMARY AND CONCLUSIONS

In this work, the thermal cycling reliability of several 2512 chip resistor lead free solder joint configurations has been investigated, with the motivation of qualifying lead free solders for harsh environment applications in ground and aerospace vehicles. In an initial study, a comparison was made between the solder joint reliabilities obtained with components fabricated with both tin-lead and pure tin solder terminations. For parts from two vendors, little difference was seen in the reliabilities for the two termination types. However, there was a noticeable difference in the reliabilities found for components from the two vendors.

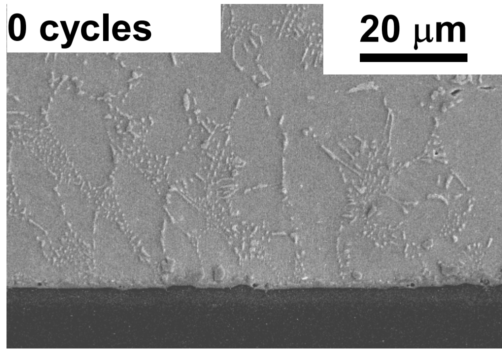

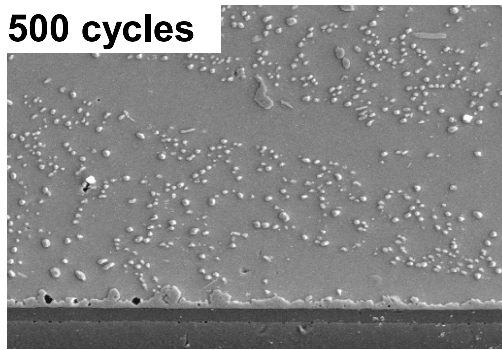

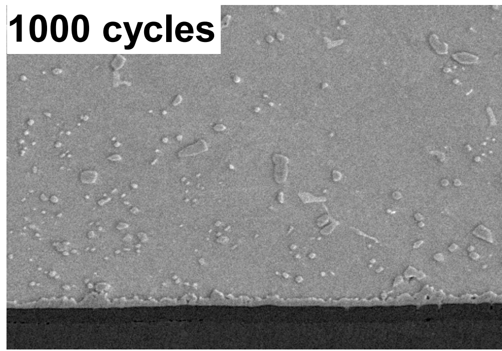

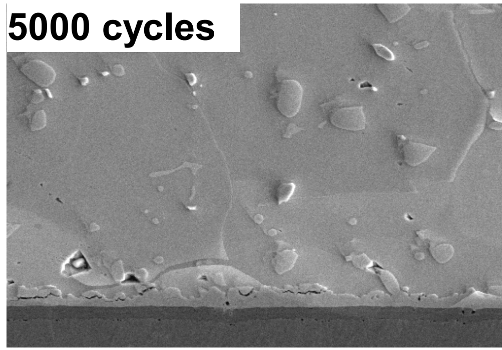

Figure 11 - SEM Images of 95.5Sn-3.8Ag-0.7Cu Joints vs. Thermal Cycling (-40 to 150 ^oC)

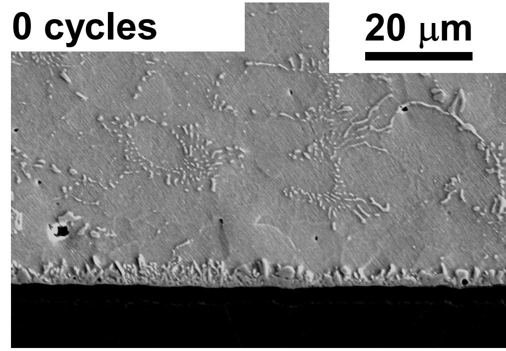

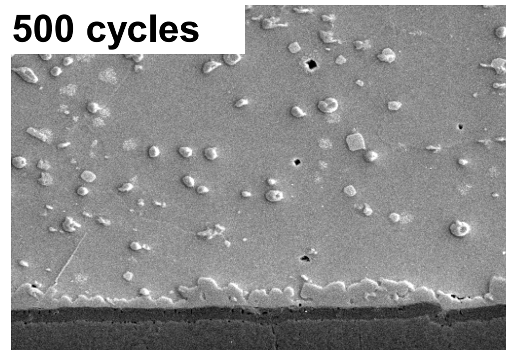

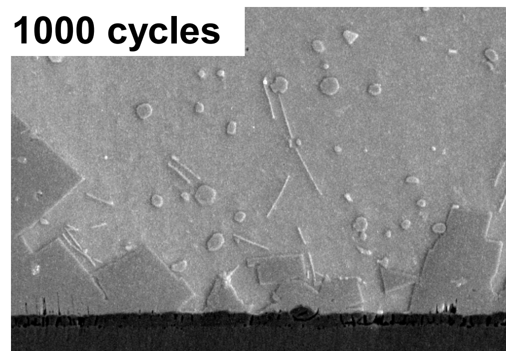

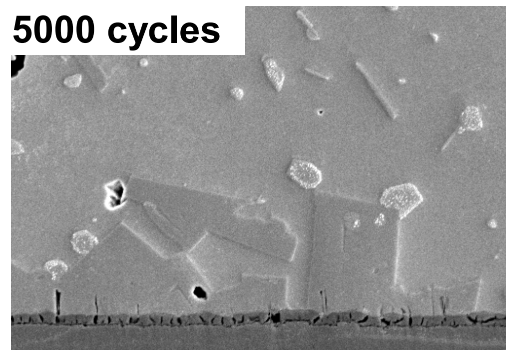

Figure 12 - SEM Images of 88.5Sn-3.0Ag-0.5Cu-8.0In Joints vs. Thermal Cycling (-40 to 150 ^oC)

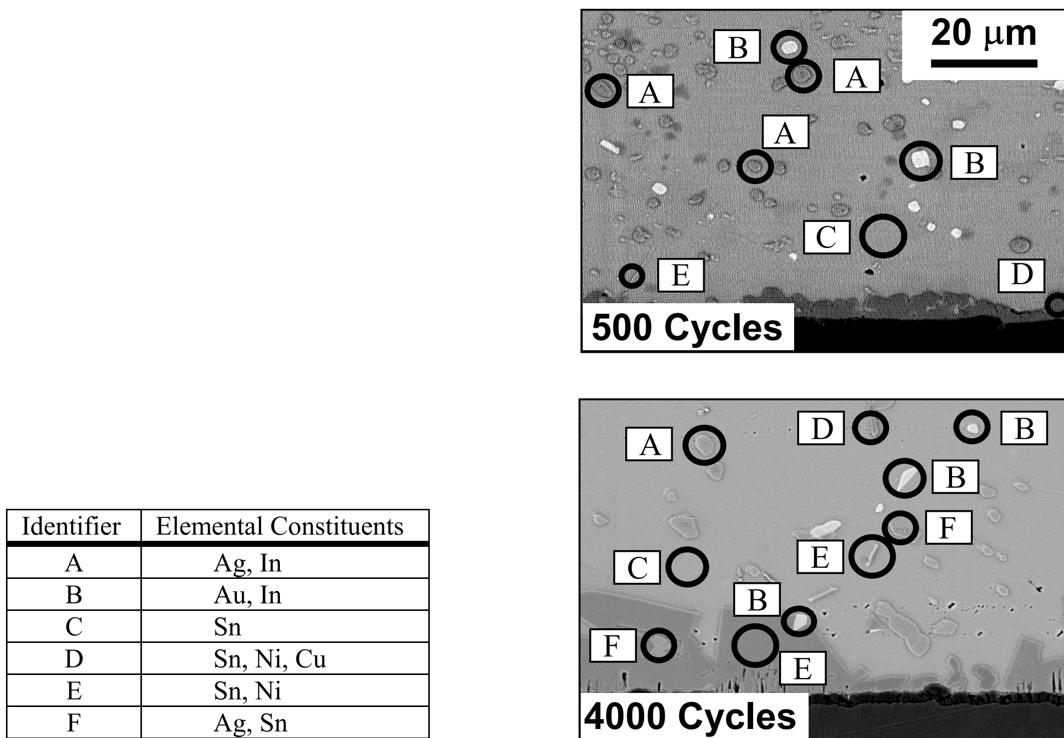

Identifier	Elemental Constituents
A	Ag, In
B	Au, In
C	Sn
D	Sn, Ni, Cu
E	Sn, Ni
F	Ag, Sn

Figure 13 - Phases and Elemental Constituents for 88.5Sn-3.0Ag-0.5Cu-8.0In Joints after 500 and 4000 Cycles

In the main portion of the experimentation, reliability testing of 2512 solder joints was performed using two temperature ranges (-40 to 125 ^{o}C and -40 to 150 ^{o}C) and five different solder alloys. The two parameter Weibull failure plots indicated that the eutectic SAC alloy (95.5Sn-3.8Ag-0.7Cu) recommended by earlier studies has similar reliability to standard 63Sn-37Pb for testing from -40 to 125 ^{o}C. However, 63Sn-37Pb joints dramatically outperformed the lead free Sn-Ag-Cu alloy joints for the more extreme -40 to 150 ^{o}C testing. This result agrees with earlier observations for CBGA and non-underfilled flip chip on laminate assemblies (configurations with high stiffness components, large CTE mismatches, and large temperature excursions). Such results further underscore the need to be cautious when proposing lead-free solder substitutions for SMT configurations in harsh environments. The measured data also indicated that quaternary variations of the lead free SAC alloy (Sn-Ag-Cu-X), which include small percentages of bismuth and indium, can be used to enhance the -40 to 150 ^{o}C thermal cycling fatigue resistance relative to standard 95.5Sn-3.8Ag-0.7Cu.

A second set of thermally cycled samples was used for microscopy studies to examine crack propagation, changes in the microstructure of the solders, and intermetallic growth at the solder to PCB pad interfaces. Failure analysis has shown that the solder joint cracking and creep-fatigue damage propagates as expected for chip resistors on FR-4 substrates. Cracks begin underneath the component and then typically follow along a path that parallels the resistor termination until complete separation has occurred. Voiding was also observed in several of the lead free solder joints, illustrating the need to further optimize the assembly process and reflow profile for each lead free solder type. This voiding is one possible explanation for the variations from linearity (waviness) and low beta values in the Weibull failure data. Another contributing factor could be material property variations. Further work is needed to fully understand the fundamental reasons for the relative reliability rankings of the solders and the Weibull slope variations.

Spheroidizing of the eutectic was observed to progress rapidly during cycling of all of the lead free alloys, and was clearly apparent in all samples after only 500 cycles. There were variations in the extent of spheroidization within each alloy and unequivocal differences in spheroidization from alloy to alloy were not apparent. It is believed that differences in the gross fillet microstructure alone do not account for the marked differences in the thermal fatigue performance of the alloys studied. A distinct difference between the alloys studied was the nature of the intermetallic layers. The intermetallic layers in the two Sn-Ag-Cu-Bi alloys and the 95.5Sn-3.8Ag-0.7Cu alloy were fairly fine (typically around 1-3 mm thick) and continuous. In contrast, the Sn-Ag-Cu-In alloy produced a highly irregular intermetallic layer consisting of large (10-20 mm) angular precipitates. Since this indium variation of the standard SAC metallurgy performed best in the -40 to 150 ^{o}C thermal cycling testing, the size and morphology of these intermetallics could be the reason for the observed differences in reliability performances of these alloys at high temperatures. However, a clear correlation was not observed between the performance of the various alloys investigated and any single microstructural feature.

ACKNOWLEDGMENTS

The work was supported by the NSF Center for Advanced Vehicle Electronics (CAVE).

REFERENCES

1. Lau, J. H., Hoo, N., Horsley, R., Smetana, J., Shangguan, D., Dauksher, W., Love, D., Menis, I. and Sullivan, B. "Reliability testing and data analysis of high-density packages' lead-free solder joints," *Proceedings of APEX 2003*, Paper S42-3, pp. 1-24, Anaheim, CA, 2003.
2. Farooq, M., Goldmann, L., Martin, G., Goldsmith, C. and Bergeron, C., "Thermo-mechanical fatigue reliability of Pb-free ceramic ball grid arrays: experimental data and lifetime prediction modeling," *Proceedings of the 53rd IEEE Electronic Components and Technology Conference*, pp. 827-833, New Orleans, LA, May 28-30, 2003.
3. Schubert, A., Dudek, R., Walter, H., Jung, E., Gollhardt, A., Michel, B., Reichl, H., "Reliability Assessment of Flip-Chip Assemblies with Lead-Free Solder Joints," *Proceedings of the 52nd Electronic Components and Technology Conference*, San Diego, CA, May 28 - 31, 2002.
4. Schubert, A., Dudek, R., Auerswald, E., Gollhardt, A., Michel, B., Reichl, H., "Fatigue Life Models for SnAgCu and SnPb Solder Joints Evaluated by Experiments and Simulation," *Proceedings of the 53rd Electronic Components and Technology Conference*, pp. 603-610, New Orleans, LA, May 28-30, 2003.
5. Stam, F. A., and Davitt, E., "Effects of Thermomechanical Cycling on Lead and Lead-Free (SnPb and SnAgCu) Surface Mount Solder Joints," *Microelectronics Reliability*, Vol. 41, pp. 1815-1822, 2001.
6. Grossmann, G., Nicoletti, G., and Soler, U., "Results of Comparative Reliability Tests on Lead-Free Solder Alloys," *Proceedings of the 52nd Electronic Components and Technology Conference*, San Diego, CA, May 28 - 31, 2002.
7. Sayama, T., Takayanagi, T., Nagai, Y., Mori, T., and Yu, Q., "Evaluation of Microstructural Evolution and Thermal Fatigue Crack Initiation in Sn-Ag-Cu Solder Joints," *Proceedings of InterPACK '03*, Paper Number IPACK2003-35096, pp.1-8, Lahaina, HI, July 6-11, 2003.